Journal of Hazardous Materials 199–200 (2012) 25–35

Contents lists available at SciVerse ScienceDirect

Journal of Hazardous Materials

journal homepage: www.elsevier.com/locate/jhazmat

Relations of As concentrations among groundwater, soil, and bedrock in Chungnam, Korea: Implications for As mobilization in groundwater according to the As-hosting mineral change

Kangjoo Kim[a,*], Seok-Hwi Kim[a], Gi Young Jeong[b,**], Rak-Hyeon Kim[c]

[a] Department of Environmental Engineering, Kunsan National University, Jeonbuk, 573-701, Republic of Korea
[b] Department of Earth and Environmental Sciences, Andong National University, Andong, Kyeongbuk, 760-749, Republic of Korea
[c] Korea Environment Corporation, Incheon, 404-708, Republic of Korea

ARTICLE INFO

Article history:
Received 23 May 2011
Received in revised form 6 October 2011
Accepted 12 October 2011
Available online 17 October 2011

Keywords:
Arsenic mobilization
As-hosting mineral
Fe-(hydr)oxides
Arsenopyrite
Pedogenetic process

ABSTRACT

Arsenic (As) concentrations and As-bearing minerals in bedrock and soil, and their relations with groundwater concentrations were investigated in a small agricultural area of Korea. The As concentration of the bedrock shows a wide variation (<0.5–3990 mg/kg) and is well correlated with that in the contacting groundwaters (23–178 μg/L). Soils, the weathering product of bedrock, show the lower and more dispersed As concentrations (8.8–387 mg/kg) than the bedrock. But the soil As concentrations are very high relative to those reported from other areas. The As concentrations in the shallow groundwaters are comparatively low (<20 μg/L) and are independent of the soil concentration. Arsenopyrite is the major As-bearing mineral in the bedrock and its oxidation controls the As levels in deep groundwater. In contrast, As mostly resides in soil as Fe-(hydr)oxide-bound forms. Due to low pH and oxidizing redox condition, the release of As from Fe-(hydr)oxides is largely suppressed, and the shallow groundwater shows low As concentrations generally satisfying the drinking water limit. However, it is suggested that the disturbance of soil geochemical conditions by land use changes would cause a serious As contamination of the shallow groundwaters.

1. Introduction

Arsenic (As) is recognized as one of the most serious inorganic contaminants in groundwater [1–3] and the As-contaminated groundwaters are observed worldwide. Although there are some anthropogenic sources, elevated As concentrations in groundwater are generally associated with geogenic sources [1,3]. For this reason, many studies focusing on the As contamination of groundwaters have also inspected As concentrations in solid phases, such as in soil, sediment, and rock (Table 1).

One of the main As sources in groundwater is sulfide minerals [1,3–7]. Some sediments and rocks containing sulfide minerals show As concentrations up to thousands of mg/kg (Table 1) due to the strong affinity of As to sulfides. Sulfide minerals occur in a variety of geological environments, but As-rich sulfides are most common in areas influenced by hydrothermal activity [3]. Sulfides are unstable in oxidizing environments and release As into water by oxidation if they contain As. Iron-(hydr)oxides are another important As host [3,8–26] because they scavenge As dissolved in natural waters [3,27]. Iron-(hydr)oxides are stable under aerobic conditions. But they dissolve in reducing environments, which frequently leads to serious As contamination in groundwater [8–24,26]. The As adsorbed onto Fe-(hydr)oxides can also be released under oxidizing conditions when the pH increases [3,25,27]. Therefore, the oxidation of As-rich sulfide minerals, the reductive dissolution of As-rich Fe-(hydr)oxides, and the desorption from Fe-(hydr)oxides are the three most common processes causing the As contamination of groundwater.

Our survey of previous studies indicates several relations for the As concentrations between groundwater and solid phases, which can be generalized based on the As source and the geochemical mechanisms causing As contamination of groundwater (Table 1). The As concentrations are generally high in solid phases where the oxidation of sulfide minerals is the major mechanism causing the groundwater contamination. In contrast, solid phases show very low As concentrations relative to the groundwater contamination level where the reductive dissolution of Fe-(hydr)oxides and/or the desorption from those phases are the major process. However, the mechanisms deriving these relations are still poorly understood.

* Corresponding author. Tel.: +82 63 469 4766; fax: +82 63 469 4964.
** Corresponding author. Tel.: +82 54 820 5619; fax: +82 54 823 1627.
E-mail addresses: kangjoo@kunsan.ac.kr (K. Kim), jearth@andong.ac.kr (G.Y. Jeong).

0304-3894/$ – see front matter © 2011 Elsevier B.V. All rights reserved.
doi:10.1016/j.jhazmat.2011.10.037

Table 1
As concentrations in groundwaters and solid phases reported in previous studies.

Location	As in bulk solids (mg/kg)	Type of solid samples	As in groundwater in contact with the solids (μg/L)	Groundwater sampling depth (m)	Major As release mechanism	Extraction method for solid analyses
Nakhon si Thammarat, Thailand [4]	<100–5000	Mining area soil	1.25–5114	No information	A	XRF
Lawrencetown, Nova Scotia, Canada [5]	Up to ca. 5000	Till, quartzite, slate	Up to 86	No information	A	HNO_3–$HClO_4$
Eastern Wisconsin, USA [6]	15–674	Sandstone, limestone, shale	Up to 12,000	No information	A	INAA
Huron County, Michigan, USA [7]	0.8–70.7	Unidentified bedrock	41–171	15–120	A	16 N HNO_3
Mankyeong River floodplain, Korea [8,9]	1.0–3.6	Gravel, sand, silt	<1–143	3.9–60	B	10 N HNO_3
Munshiganj, Bangladesh [10]	0.5–8	Sand, clay	Up to 640	5–165	B	16 N HNO_3 + H_2O_2
Chapai-Nawabganj, Manikganj, and Chandpur, Bangladesh [11]	<1–11	Sand, clay	3.02–315	15–66	B	XRF
Chandpur, Bangladesh [12]	3.6–17.3	Silt, clay, sand	6–934	15–150	B	XRF
Barasat, West Bengal, India [13]	0.52–4.48	Silt, clay, sand	0.82–538	15–82	B (C[b])	No information
Baruipur, West Bengal, India [14,15]	34 ± 2.46	Silt, clay, sand	0.77–1059	14–305	B	16 N HNO_3
Holocene Terai Basin, Nepal [16]	2–31	Gravel, sand, silt, clay	<10–740	<26	B	XRF
Red River Delta, Vietnam [17]	<5–22	Gravel, sand, silt, clay	<1–340	9–100	B	16 N HNO_3 + H_2O_2
Huhhot Basin, China [18]	3–29	Sand, silt, clay	<1–1480	4–400	B	HNO_3–$HClO_4$–HF
Hetao Basin, China [19]	7–73	Sand, silt, clay	0.6–572	5–80	B	HNO_3–$HClO_4$–HF
Chianan Coastal Plain, Taiwan [20,21]	Up to 30	Silt, clay, sand	Up to 12,000	<300	B	0.5 M H_3PO_4 + 0.1 M $NH_2OH{\cdot}HCl$
Chapai-Nawabganj, Bangladesh [22]	1–55	Sand, silt	2.8–462	10–40	B	XRF
Mekong River Delta, Vietnam [23]	4–45	Gravel, grit, sand, silt, clay	1–741	20–440	B (A[b])	XRF
Southern Carson Desert, Nevada, USA [24]	0.7–10	Sand, clay, volcanic ash	11–2620	2.7–14.3	B, C	0.04 M NH_2OH + HCl + CH_3COOH
Santiago del Estero, Argentina [25]	2.5–7.3	Gravel, sand, silt, clay	7.0–14,969	3–12	C	7 N HNO_3
This study	8.8–387	Soil	<1–16[a]	<20	D	10 N HNO_3
	2.1–3990	Rock core	23–178[a]	100–150	A	INAA, 10 N HNO_3

A: oxidation of As-rich sulfides, B: reductive dissolution of Fe or Mn (hydr)oxides, C: desorption from Fe (hydr)oxides, D: no As release by adsorption onto Fe (hydr)oxides,
[a] Based on old wells.
[b] Minor mechanism.

In this study, As concentrations in bedrock and its weathering product, soil, and their relations with groundwater concentrations were systematically investigated in a small village of Chungnam Province, Korea (Fig. 1). This study was performed to explore the relations of As concentrations among rocks, soils, and groundwaters, and, thus, to understand the governing processes controlling their relations and the mobilization of As in groundwater under different geochemical conditions. In the study area, the weathering of As-rich rocks caused the serious soil contamination. However, the As concentrations of the shallow groundwaters in the study area are very low relative to the soil As levels. Therefore, the area can provide valuable insights into the relations between groundwater and contacting solid phases and into the processes controlling As mobilization in groundwater.

2. Study area

The study area is characterized by metasedimentary rocks of unknown age (Majeonri Formation, Changri Formation) intruded by Mesozoic to Cenozoic plutonic rocks, which include granite and quartz porphyry (Fig. 1a) [28]. The village where this study was performed is located in the Majeonri Formation area, which consists of calcareous sedimentary rocks such as limestone, calcareous sandstone, and calcareous slate [28]. Regional tectonic deformation of the Majeonri Formation has resulted in the development of numerous fissures, which are commonly filled with calcite, quartz, and pyrite (FeS_2) veins. However, some sets of veins are enriched with arsenopyrite (FeAsS) and other sulfide minerals in addition to pyrite. Yellow-brown precipitates of Fe-sulfates were found coating the weathered surfaces of the arseonopyrite–pyrite–calcite–quartz veins exposed on the roadcut. The veins of the Majeonri Formation were formed certainly by multiple stages of tectonic deformation through the long geological time. The arsenopyrite-bearing veins are distinguished from others in their hydrothermal mineralogy such as sphalerite (ZnS), chalcopyrite ($CuFeS_2$), and galena (PbS) (Appendix Fig. S1). The Changri Formation is found at the northwestern end of the village and is composed of blackish or greenish schist, phyllite, and slate with intercalated limestones [28].

The village where this study was performed is surrounded by mountains with elevations ranging from 400 to 600 m above the mean sea level (a.m.s.l.). The elevation in the eastern side of the village is higher than that in the western side by 30–40 m and there is a small stream (140–150 m a.m.s.l.) flowing from the north through the western side of the village. Water table depths from the land surface vary within a narrow range (1.1–5.0 m with 2.9 m in average; Table 2) relative to the variation of land elevation, indicating

Table 2
Chemical analysis data for groundwater samples.

ID	Sampling time	Well depth (m)	Water table[a] (m)	pH	EC (μS/cm)	DO (mg/L)	Temp (°C)	Eh (mV)	Alk (mN)	Cl (mg/L)	NO_3 (mg/L)	SO_4 (mg/L)	Na (mg/L)	Mg (mg/L)	K (mg/L)	Ca (mg/L)	Fe_T (μg/L)	As_T (μg/L)	As(III) (μg/L)	$\delta^{18}O$ (‰)	δD (‰)
(A) Old wells																					
BG5	A	130	–	7.42	229	7.84	17.0	447	1.72	3.81	9.23	14.3	6.80	6.29	2.86	28.7	11.7	90	–	–	–
BS4	A	13.9	3.85	6.57	474	3.31	15.9	389	3.15	16.2	24.6	27.4	6.52	6.60	2.56	81.2	19.3	4	–	–	–
BS5	A	14.6	2.51	6.97	403	3.68	15.5	485	3.73	15.1	25.1	20.5	5.99	5.74	2.43	84.4	19.4	7	–	–	–
BS6	A	10.2	1.37	7.67	402	6.49	16.0	449	3.09	8.07	18.7	18.7	4.96	4.52	2.02	66.6	19.2	5	–	–	–
BS7	A	17.0	3.45	6.99	542	3.16	15.3	448	4.23	15.3	25.6	20.5	6.92	6.13	3.13	92.3	13.9	14	–	–	–
BS8	A	11.1	3.29	6.92	428	3.80	17.4	466	3.49	14.4	29.3	17.2	5.22	5.57	2.12	78.6	15.7	3	–	–	–
BS9	A	3.1	2.39	6.38	453	4.90	18.9	465	2.71	19.2	32.4	42.9	8.18	7.43	5.85	69.1	65.7	5	–	–	–
BS10	A	2.1	1.81	5.93	403	5.73	17.2	307	1.48	5.43	22.6	67.1	5.44	7.72	6.20	42.4	28.7	<1	–	–	–
BS19	A	150	2.59	7.58	218	0.73	14.7	302	1.63	8.06	8.59	24.1	12.5	3.53	2.43	35.4	17.0	138	–	–	–
BG5	B	130	–	7.76	218	7.89	16.2	188	1.78	3.57	6.68	14.3	6.77	6.11	2.65	28.1	11.5	93	–	−8.88	−63.3
BS4	B	13.9	3.40	7.20	482	3.66	15.2	314	3.50	15.9	25.7	28.4	6.26	6.70	2.56	78.3	114	6	–	−8.37	−61.6
BS5	B	14.6	4.14	7.25	484	4.44	14.6	314	3.63	15.5	23.8	21.5	5.88	5.90	2.43	76.0	130	7	–	−8.55	−62.1
BS6	B	10.2	2.30	7.12	377	7.34	17.7	211	2.90	4.84	16.3	20.2	4.31	4.34	2.02	61.9	11.0	4	–	−8.97	−63.8
BS7	B	17.0	1.13	7.24	545	3.77	17.1	219	4.49	1.82	22.7	20.0	6.40	6.13	2.87	87.0	9.04	14	–	−8.68	−62.2
BS8	B	11.1	4.21	7.35	477	4.14	14.5	305	3.63	14.9	27.4	18.3	5.16	5.68	2.13	82.8	122	3	–	−8.56	−61.8
BS9	B	3.1	–	7.13	480	6.04	20.8	229	3.67	12.1	20.5	35.2	7.27	6.47	4.89	79.7	27.4	7	–	−8.73	−62.8
BS10	B	2.09	1.70	6.20	380	5.78	19.9	219	1.75	5.41	25.6	71.7	5.53	7.81	10.7	52.5	44.0	<1	–	−9.50	−67.1
BS11	B	145	–	7.82	293	6.74	17.2	284	1.54	4.67	12.6	11.0	6.08	5.02	1.78	28.4	55.2	88	–	−9.01	−64.6
BS12	B	10.0	–	6.76	364	4.57	18.3	284	2.34	3.25	9.18	20.0	8.19	4.60	4.30	40.3	54.9	3	–	−9.52	−66.4
BS13	B	–	–	7.75	233	5.84	18.6	443	1.90	3.25	4.93	13.0	3.22	6.45	2.82	29.6	125	68	–	−8.96	−64.7
BS19	B	150	–	7.79	251	2.77	15.9	176	1.61	7.82	12.7	19.7	10.4	3.49	2.64	34.1	26.0	178	–	−8.99	−63.5
BG5	C	130	–	7.63	270	5.89	15.3	364	1.84	4.65	8.37	20.1	7.46	6.57	2.91	33.6	45.1	96	<1	−8.84	−62.4
BS4	C	13.9	3.62	7.21	503	2.82	15.0	307	3.45	16.0	30.1	28.5	6.71	6.82	2.56	81.5	10.0	6	<1	−8.40	−60.0
BS5	C	14.6	–	7.16	495	3.34	14.4	475	3.74	14.9	25.3	19.3	5.87	5.69	2.27	78.9	60.5	6	<1	−8.47	−60.4
BS6	C	10.2	2.83	7.18	435	6.87	14.3	388	3.32	9.42	19.7	16.0	5.15	4.85	2.11	77.5	9.57	6	<1	−8.51	−60.8
BS7	C	17.0	5.01	7.04	524	4.10	15.0	480	4.04	14.7	29.0	20.0	6.69	5.86	3.06	91.0	18.5	16	<1	−8.54	−60.8
BS8	C	11.10	–	7.23	482	4.47	14.5	383	3.44	14.4	30.2	15.2	5.03	5.54	2.06	82.6	8.88	3	<1	−8.54	−60.2
BS9	C	3.1	–	6.96	553	5.79	15.7	391	3.21	18.3	34.8	33.6	8.49	7.07	4.05	91.9	3.37	11	<1	−8.13	−58.3
BS11	C	145	–	7.74	302	9.99	15.0	370	2.09	6.56	22.0	13.4	8.41	5.19	1.73	42.5	3.06	117	<1	−8.83	−62.4
BS12	C	10.0	–	6.66	370	5.50	15.1	410	3.06	4.35	5.16	23.3	2.61	4.27	1.18	63.1	62.2	<1	<1	−8.88	−61.6
BS13	C	–	–	7.73	271	7.81	15.6	372	1.87	4.80	7.63	21.0	7.63	6.71	2.88	32.4	29.3	93	<1	–	–
(B) New well																					
NW1	C	9.4[b]	–	7.79	329	6.04	17.6	371	2.67	6.19	9.90	19.3	6.08	4.93	2.47	47.8	33.7	36	1	–	–
NW2	C	13.0[b]	–	7.65	322	7.45	14.7	372	2.64	5.04	8.90	16.2	5.63	4.63	2.39	48.2	25.7	38	<1	–	–
NW3	C	15.1[b]	–	7.62	298	6.42	15.4	339	2.59	3.70	6.37	10.7	4.82	5.05	2.53	45.3	37.0	29	1	−8.72	−60.9
NW4	C	15.4[b]	–	7.76	291	5.84	17.7	367	2.56	3.78	6.61	11.5	5.27	4.77	2.63	44.2	132	34	1	–	–
NW5	C	20.1[b]	–	7.94	303	2.66	17.0	189	2.69	3.11	3.25	12.8	6.00	6.22	2.70	43.7	28.7	29	2	−8.79	−61.4
NW6	C	20.4[b]	–	7.79	299	5.35	16.7	345	2.67	3.78	5.93	12.3	5.00	5.05	2.51	44.4	37.1	30	2	–	–
NW7	C	25.1[b]	–	7.96	286	2.45	15.7	264	2.45	3.56	3.73	13.2	6.92	5.82	3.24	40.4	38.2	37	25	−8.83	−61.8
NW8	C	29.6[b]	–	7.96	261	2.43	16.9	299	2.24	3.06	3.23	12.0	7.68	5.89	3.18	33.9	40.0	40	7	−8.85	−62.1
NW9	C	63.9[b]	–	7.84	307	5.64	16.6	375	2.60	4.17	6.72	13.4	5.60	5.18	2.52	45.0	11.0	34	<1	–	–
NW10	C	66.0[b]	–	7.95	296	1.07	17.1	289	2.38	4.24	4.39	18.9	8.22	5.93	3.08	40.8	28.8	22	<1	−8.81	−61.9
NW11	C	71.0[b]	–	7.91	296	1.64	15.8	406	2.41	4.26	4.25	19.5	9.34	6.68	3.13	38.7	24.8	31	3	−8.81	−61.2
NW12	C	119.5[b]	–	7.65	306	1.74	16.8	291	2.15	3.62	4.05	15.9	7.33	5.82	3.08	44.8	37.4	27	2	−8.78	−61.5
NW13	C	129.7[b]	–	7.91	233	2.57	18.5	269	1.74	3.56	0.50	17.2	24.9	2.29	1.53	20.0	79.7	62	55	−8.91	−62.8
NW14	C	131.8[b]	–	8.18	258	0.68	16.4	336	2.06	3.66	1.38	18.9	23.3	3.11	2.04	26.0	160	48	4	–	–
NW15	C	136.8[b]	–	8.05	285	0.71	16.5	425	2.27	3.90	3.00	19.3	17.5	4.17	2.50	32.7	33.0	39	5	–	–
NW16	C	139.7[b]	–	8.12	217	1.03	18.6	158	1.49	3.48	<0.1	18.3	26.0	1.50	1.26	14.9	37.3	375	304	−8.93	−62.7

A: July 24–27, 2007, B: September 6–10, 2007, C: May 30–June 1, 2008.

[a] Depth to the water table from the land surface.

[b] Groundwater sampling depth.

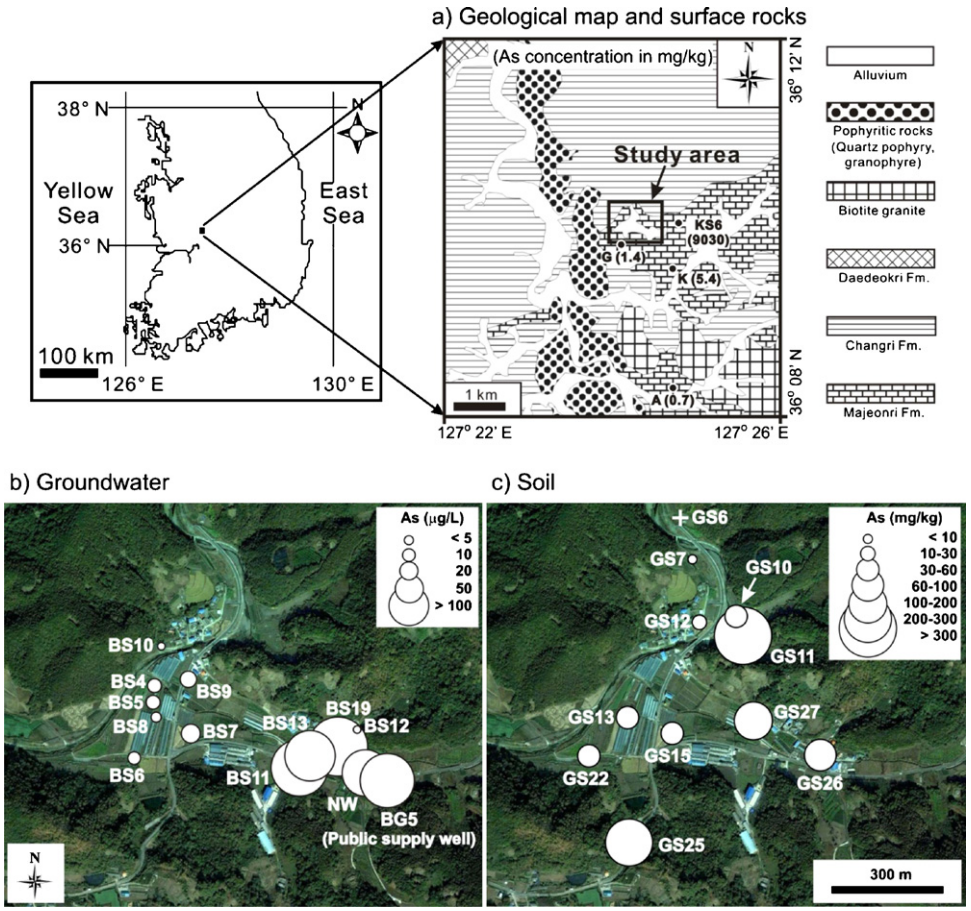

Fig. 1. Geological map of the study area and the As concentrations in outcrop samples (a), the As concentrations in groundwater (b) and soil (c).

that the water table configuration generally follows the land relief [29]. Considering this, the groundwater in the village is likely to flow westward from the east and discharges into the stream in overall (Fig. 1b).

The soils in the study area are 2–5 m thick and classified as inceptisols having good soil drainage [30]. The land within and around the village is mainly used for cultivation of paddy and vegetables such as reddish, cabbage, lettuce etc., with scattered residences. The climatological record for the past 30 years indicates that the annual average precipitation is 1300 mm, of which more than 70% occurs from June till September [31]. The mean monthly air temperature is highest in August (24.7 °C) and lowest in January (−2.9 °C).

3. Materials and methods

3.1. Groundwater sampling and analysis

For this study, eleven private wells (mostly 2–150 m in depth with two depth-unknown wells) and one public water supply well (130 m in depth) were investigated (Fig. 1; Table 2). Thirty-one groundwater samples were collected in total from those wells during three sampling campaigns from 2007 to 2008 (Table 2). An additional well (150 m in depth) was installed as a part of this study during October of 2007 near the wells with high As concentrations: this well is referred to as a 'new well', and the other wells are referred to as 'old wells'. Most of the wells used for this study have short casings (<10 m) at shallow depth, and the remaining parts were left open to the bedrock aquifer. Sixteen groundwater samples were collected from various depths of the new well by isolating the depth intervals (5–10 m) using a double packer. However, the packer was not used for sampling the old wells. The water samples were collected after purging at least three well volumes or until DO, Eh, pH, and EC became stable. The well purging and groundwater sampling were performed using submersible pumps for old wells and using a Waterra pump for the new well.

The water samples for lab analysis were filtered immediately onsite through 0.45 μm membrane using syringes. Each sample bottle was washed three times with the filtrates before sampling. The samples (100 mL) for major cations (Ca^{2+}, Mg^{2+}, Na^{+}, K^{+}), Fe_T and As_T were acidified with concentrated HNO_3 to a pH < 2. The non-acidified fraction (100 mL) was collected for the measurement of anions (Cl^{-}, SO_4^{2-}, NO_3^{-}) and alkalinity. In this study, isotopic compositions and As(III) concentrations were analyzed to get information for the water origins and for the As behavior, respectively. These analyses were performed for selected samples taken during the second and third sampling campaigns (Table 2). As(III) samples (30 mL) were collected by filtering the water sample through a 0.45 μm membrane filter and then a disposable anion exchange cartridge at a flow rate of approximately 6 mL/min using a syringe. The cartridge contained 0.8 g aluminosilicate adsorbent that selectively adsorbs As(V) but not As(III) [32]. The As(III) samples were also acidified to pH < 2. The isotope samples for analysis of oxygen and hydrogen isotopes (50 mL) were unfiltered, and the bottles were sealed with parafilm tape to prevent potential isotope fractionation [33]. All the water samples were kept at 4 °C till analysis.

DO, Eh, pH, and EC were measured in the field using a flow-through chamber to minimize the disturbance by contacting with air. Electrodes of Eh, pH, and EC were calibrated using

Zobel solution, standard pH buffer solutions, and standard EC solutions, respectively. Alkalinity was determined based on the Gran titration technique [34]. Major cations were analyzed using a flame atomic adsorption spectroscopy (AAS; Varian AA240FS); Fe_T using graphite furnace AAS (Varian AA240FS-GTA120); As_T and As(III) using the flame AAS with a hydride generator; and major anions using ion chromatography (Dionex DX500). The oxygen and hydrogen isotopes ($\delta^{18}O$ and δD) were analyzed using a mass spectrometer (Micromass Optima) at the Korea Basic Science Institute. The analytical results show ion balance errors within ±5% for all the groundwater samples. The computer code PHREEQC [35] was used to calculate the saturation indices of calcite ($SI_{calcite}$) and pCO_2 (log partial pressure of CO_2 in atm).

3.2. Rock and soil sampling and analysis

A 150 m long bedrock core was retrieved while installing the new well. Surface rock samples (~1 kg) were collected from the outcrops around the village (Fig. 1a). Soil samples (~1 kg) were collected from the land surface (<15 cm in depth) (Fig. 1c), stored in plastic bags, and air-dried on arriving at the laboratory. The sampling times for solid samples are indicated in Table 3.

The microscopic occurrence of As-bearing minerals in the rock and soils was investigated using a scanning electron microscope (SEM; JEOL JSM 6300) equipped with an Oxford energy dispersive X-ray spectrometer (EDS). For SEM analysis, fragments taken from the rock samples were coated with gold and observed in the secondary electron imaging mode. Polished thin sections prepared from the rock and soil samples after epoxy impregnation were observed in the back-scattered electron (BSE) imaging mode. The As contents of the minerals in the polished thin sections were measured using an electron microprobe analyzer (Shimadzu 1500). Fine particles of yellow-brown coatings were dispersed in methanol, and loaded on a micro-grid to observe their morphology, chemistry, and structures using a transmission electron microscope (JEOL JEM2010).

For mineralogical investigation of core samples, 24 subsamples were selected from the core based on bare-eye and loupe inspections. The major criterion for the selection of the 24 subsamples was the presence of sulfide-rich veins because our petrographic analysis confirmed the absence of arsenopyrite in the host rocks. However, we also considered the sampling intervals during the collection to minimize the bias problem (Table 2).

Because each study applies different methods for analysis of bulk As concentrations in solid phases (Table 1) and the results are dependent on the analytical methods, it is sometimes difficult to compare the As concentrations directly with those of other studies. Therefore, the bulk As concentrations in rock samples were analyzed using two different methods: (i) instrumental neutron activation analysis (INAA) and (ii) 10 N HNO_3 extraction method. The former was applied for the outcrop samples and the 24 subsamples of the rock core and the latter was applied for the 15 subsamples, which were additionally collected from the core with a regular depth interval (10 m) to compensate for the bias problem associated with the selective collection. The INAA was performed by the Activation Laboratories Ltd., Canada. For the HNO_3 extraction analysis, 0.5 g of the pulverized rock sample was extracted using 25 mL of 10 N HNO_3 at 105 °C for 1 h in an autoclave. The As concentrations in the extractants were analyzed using the method applied for groundwater analysis. The bulk As concentrations in the soil samples were analyzed using the same HNO_3 extraction scheme. For this analysis, the air-dried soil samples were pulverized.

Table 3
As concentrations in solid samples (mg/kg).

Soil samples (May 30–June 1, 2008)		Core samples (October 3–13, 2007)			
ID	10 N HNO_3 extraction	Depth (m)	10 N HNO_3 extraction	Depth (m)	INAA
GS6	NA	10.0	0.9	4.1	5.9
GS7	8.8	20.0	3.4	7.7	<0.5
GS10	47.5	30.0	0.6	19.1	<0.5
GS11	387	40.0	2.7	38.9	2.9
GS12	13.0	50.0	0.8	48.7	4.6
GS13	37.1	60.0	6.8	54.1	10.6
GS15	45.8	70.0	4.8	58.7	29.4
GS22	41.4	80.0	0.8	68.2	<0.5
GS25	249	90.0	20.6	79.3	2.9
GS26	68.7	100.0	3.2	82.4	1.1
GS27	183	110.0	3.5	89.3	<0.5
		120.0	2. 8	98.1	1.8
		130.0	2.1	101.7	5.8
		140.0	10.8	105.8	1.9
		150.0	2471	110.7	<0.5
				114.8	3990
				117.7	6.4
				122.8	19.0
				130.4	9.0
				135.8	25.0
				139.7	25.0
				146.8	2.2
				149.5	138
				150.0	2580

Surface rock samples (September 6, 2007)	
ID	INAA
A	0.7
G	1.4
K	5.4
KS6	9030

NA: not analyzed.

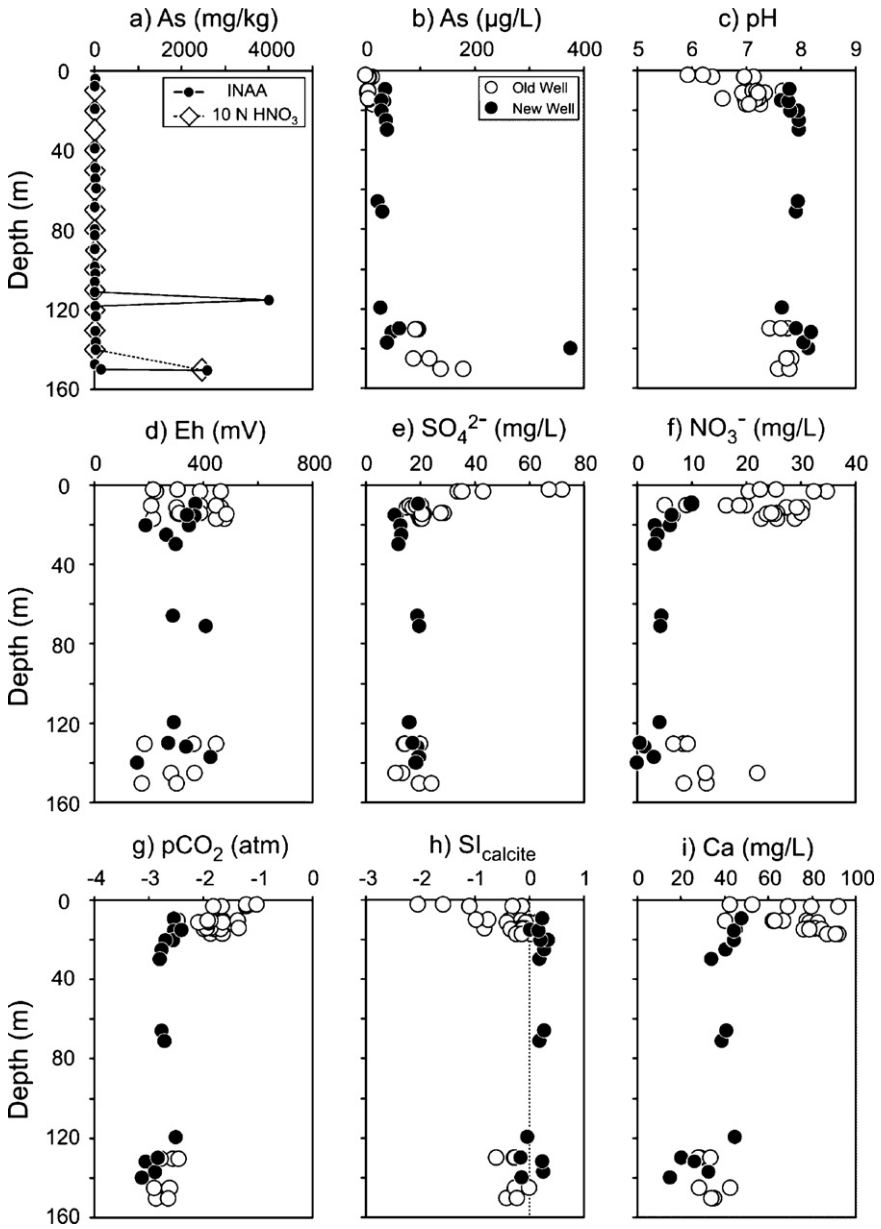

Fig. 2. Vertical profiles for As in rock core (a) and for groundwater chemistry (b–j). $SI_{calcite}$ represents saturation index of calcite.

4. Results and discussion

4.1. As concentration and source of groundwater

The old wells show As_T concentrations ranging from <1 μg/L to 178 μg/L (32 μg/L on average; Table 2). The public supply well showed As_T concentrations fluctuating between 90 and 96 μg/L during the three sampling campaigns. The wells with As_T concentrations >50 μg/L are located adjacent to the public supply well (Fig. 1) and have depths between 120 and 150 m (Table 2). The average As_T concentration was 5.9 μg/L if only wells with depths <20 m were considered. The As_T concentrations in the new well show a similar vertical variation to those observed from the old wells (Fig. 2b). New well samples show As_T concentrations of 57.0 μg/L on average. The highest concentration of the new well (375 μg/L) was observed in the depth of 140 m.

The isotope data for $\delta^{18}O$ and δD are plotted along the global meteoric water line (GMWL; Fig. 3), indicating that the precipitation is the essential groundwater source [34]. The deep groundwaters with high As concentrations generally show lighter isotopic compositions than the shallow groundwaters, which illustrates that the former were recharged from higher altitudes and circulate deeply and the latter were recharged in the area around the wells [33,36,37]. Some shallow wells located on the mountain foot slopes (BS10, BS12) showed much lighter isotopic compositions than the other wells during the summer rainy season, most likely due to the infiltration of overland flows coming from high altitudes at the mountain foot as the slope decreases (Fig. 3).

4.2. Rock mineralogy and As concentration

Mineralogical analysis of the thin sections showed that fissure-filling veins were common throughout the core samples (Fig. S2 of Appendix). Several types of veins were observed from the core sample: calcite, quartz, calcite–pyrite, quartz–calcite, quartz–pyrite, calcite–pyrite–amphibole, pyrite–arsenopyrite, and calcite–pyrite–arsenopyrite. Arsenopyrite-bearing veins were common in the lower part of the core, particularly at depths of 115

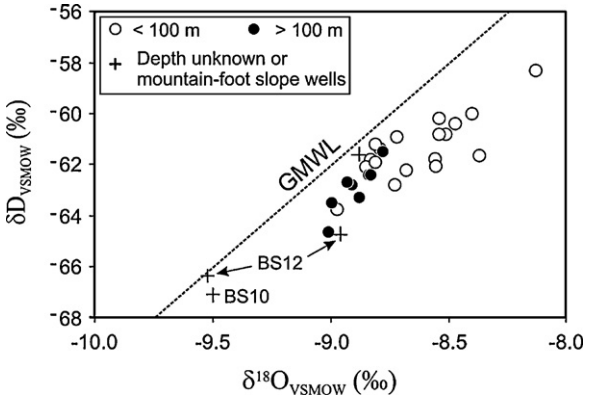

Fig. 3. The relation between $\delta^{18}O$ and δD for groundwater samples.

and 150 m (Fig. 4a–d). Pyrite was frequently observed in most of the core samples. However, As was not detected in pyrite by EDS analysis.

Schwertmannite were observed in the secondary yellow-brown coatings on the surfaces of the sulfide veins exposed on a 10 year-old roadcut. The rock sample KS6 was also collected from this roadcut (Fig. 1a). The pyrite shows a corrosion texture by dissolution (Fig. 5a), and the interstices were filled with Fe-sulfates (Fig. 5b). TEM analysis of the extracted Fe-sulfates showed a typical pin-cushion morphology of schwertmannite (Fig. 5c) [38], which was confirmed by electron diffraction and EDS analysis. Arsenopyrite crystals were associated with pyrite in the fresh part of the veins (Fig. 5d). Schwertmannite is a transient phase normally formed by the oxidation of sulfide minerals in acidic environments and is known to transform into Fe-(hydr)oxides as the solution pH increases [39]. The As contents were high in the schwertmannite (0.19–0.68 wt%), which indicates that the As released from arsenopyrite by weathering was temporarily adsorbed on the surface of schwertmannite or incorporated into the schwertmannite structure [40–42].

The INAA data for the surface rock samples collected from the outcrops of the Majeonri Formation show a wide range of bulk As concentrations (Fig. 1a; Table 3). The highest As concentration (9030 mg/kg) was observed in the sample bearing arsenopyrite-rich veins (KS6). However, other outcrop samples showed As concentrations <5.4 mg/kg and arsenopyrite was not observed even though they contain pyrite veins. The As contents in the rock core also vary widely from <0.5 to 3990 mg/kg (Fig. 2a; Table 3). The As concentrations higher than 1000 mg/kg were observed in the samples collected from the depths of 114.8 (3990 mg/kg) and 150.0 m (2580 mg/kg) where arsenopyrite-bearing veins were observed, indicating that the occurrence of arsenopyrite regulates the bulk As concentrations in rocks. The next highest As concentration was observed at 149.5 m in depth (138 mg/kg). Other samples showed concentrations ranging from <0.5 to 29.4 mg/kg.

The 10 N HNO_3 extraction results for the core samples show that the vertical As variation is similar to that of the INAA data (Fig. 2a; Table 3). The slight differences seem to be associated with the depth differences of the analyzed samples except one collected from 150 m. The highest As concentration from the HNO_3 extraction was observed at a depth of 150.0 m (2471 mg/kg) and is nearly identical to that analyzed based on the INAA. The similar results of both analytical methods for the same sample are associated with the facts that the concentrated HNO_3 can dissolve carbonates, metal (hydr)oxides, and sulfides and that the As is mostly associated with sulfide minerals in the rocks.

4.3. Soil mineralogy and As concentration

The microtextural and mineralogical investigation revealed that Fe-(hydr)oxides are the most important mineral phases hosting As in the soils. The soils in the study area show a granular structure with granules approximately 1 mm in diameter (Fig. 6a). The bright parts of the BSE images display the location of Fe-rich minerals, showing that the Fe is not homogeneously distributed. In Fe-rich granules, the Fe precipitates form colloform and concentric aggregates (Fig. 6c, d and g) that are often mixed with detrital mineral particles such as quartz, feldspars, and micas (Fig. 6b, f, h and i). The

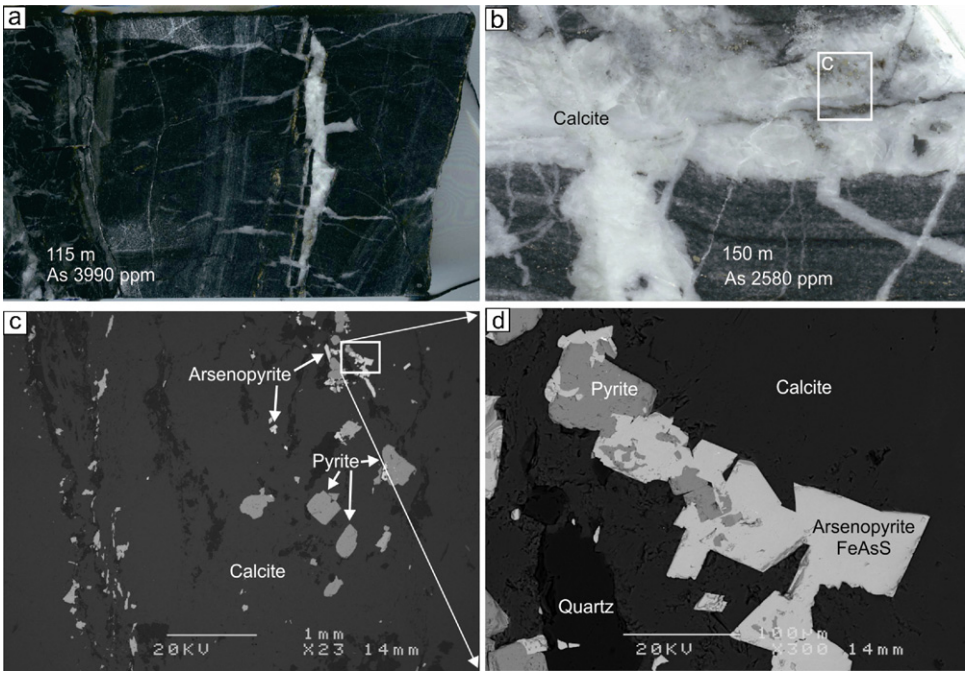

Fig. 4. Photomicrographs of core samples collected from depths of 115 m (a) and 150 m (b) showing fissures filled with hydrothermal minerals. SEM images of the core sample (b) show the occurrence of pyrite and arsenopyrite crystals in the calcite veins (c and d).

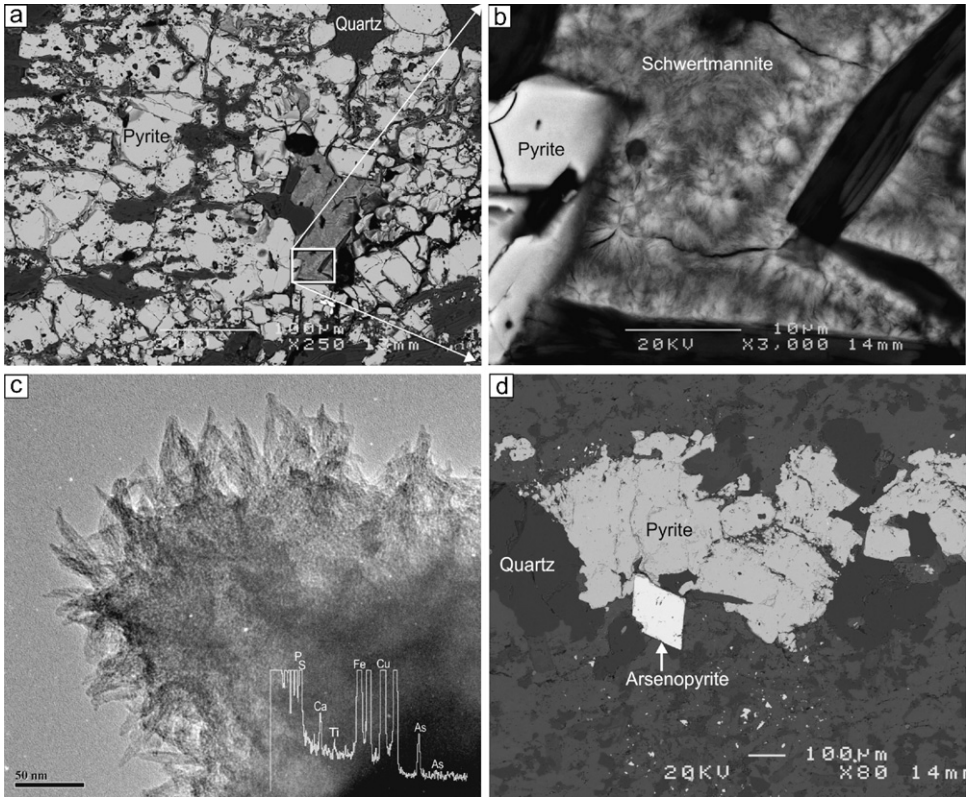

Fig. 5. BSE images of fibrous schwertmannite filling the dissolution voids of pyrite (a and b) in weathered sulfide veins exposed on the recent roadcut. The TEM image and EDS spectrum of As-bearing schwertmannite (c) and the BSE image of arsenopyrite in the fresh part of the vein (d).

mineralogical nature of the Fe aggregates was not directly determined due to their small contents and sizes. The negligible sulfur contents from EDS analysis (Fig. 6), however, indicates that they are not schwertmannite but Fe-(hydr)oxides. The Fe-(hydr)oxides frequently contain As, as shown by the EDS analysis (Fig. 6c, d and f), even though some show very low As content (Fig. 6g, h and i). The electron microprobe analysis indicates that the Fe-(hydr)oxides contain As concentrations up to 6.59 wt% (Table 4).

The colloform Fe-(hydr)oxide aggregates were well-developed and the inclusions of detrital particles were rarely observed (Figs. 6c, d and g). This occurrence of the colloform Fe granules in the soils indicates that they are the fragments of Fe precipitates forming at the site of oxidative sulfide weathering in the bedrock-soil transient zone. The colloform aggregates of Fe-(hydr)oxides were detached from the site of sulfide weathering and were mechanically mixed into the soil by pedogenetic processes, including the activity of soil biomass, burrowing, mass wasting, and cultivation. Arsenopyrite-bearing sulfide veins, such as those in Figs. 4 and 5, are locally distributed in the bedrocks of the area. The weathering of these veins results in local formation of the colloform mass of As-bearing Fe-(hydr)oxides followed by subsequent dispersion by pedogenetic processes. However, we cannot completely exclude the possibility of the weathering of As-rich sulfides, which were mechanically moved and mixed into the soil. In any case, the pedogenetic process played an important role in spreading the soil As contamination.

The soils of this study area show As concentrations higher than any other soils and sediments reported from the areas where the

Table 4
Microprobe analysis data for Fe (hydr)oxides in selected soil samples (wt%).

	GS6				GS11		GS15	GS25		
	1	2	4	5	1	2		1	2	3
Al_2O_3	0.20	0.27	6.31	6.86	7.70	1.21	3.78	1.48	0.80	0.54
P_2O_5	0.03	0.02	0.39	0.58	0.50	0.09	0.25	0.13	0.15	0.13
SO_3	0.05	0.08	0.10	0.08	0.48	0.02	0.11	0.00	0.03	0.04
FeO	68.76	67.93	46.88	61.33	44.93	68.46	60.75	66.35	67.05	71.07
As_2O_3	0.01	0.00	0.63	0.20	8.70	0.41	1.52	0.92	0.80	0.11
Total	69.05	68.31	54.31	69.04	62.31	70.19	66.40	68.88	68.83	71.89
Al	0.15	0.20	4.78	5.19	5.83	0.92	2.86	1.12	0.60	0.41
P	0.01	0.01	0.17	0.25	0.22	0.04	0.11	0.06	0.07	0.06
S	0.02	0.03	0.04	0.03	0.19	0.01	0.04	0.00	0.01	0.01
Fe	53.45	52.81	36.44	47.67	34.92	53.22	47.22	51.57	52.12	55.24
As	0.01	0.00	0.47	0.15	6.59	0.31	1.15	0.69	0.61	0.09
Total	53.64	53.05	41.91	53.30	47.75	54.49	51.38	53.45	53.41	55.81

Here, totals of oxides are much less than 100% because Fe-(hydr)oxides normally contain water in their structure and occur as aggregates bearing micropores.

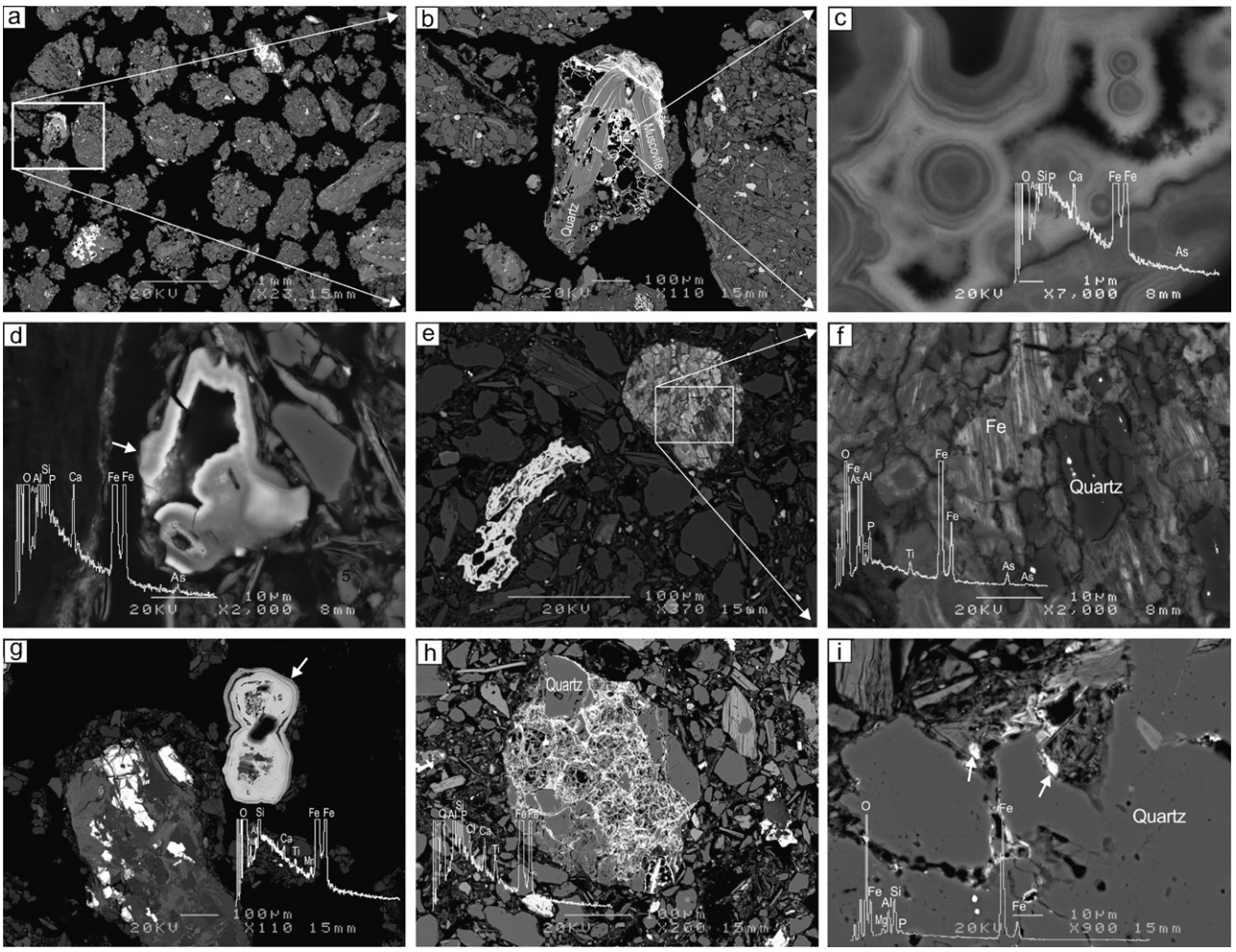

Fig. 6. Microscopic occurrences of As-bearing Fe (hydr)oxides in the study area. BSE image of a thin section of soil shows a granular structure (a). The Fe-rich regions are indicated by the bright contrast. The black areas are epoxy resin. As-bearing iron (hydr)oxides form concentric colloform aggregates (b–d) in the soil granules or mixtures with detrital mineral particles (b, e and f). Some of the Fe (hydr)oxides in the colloform concretion (g) and the mixed granules (h and i) show As contents below the detection limit. The EDS spectra added to the BSE micrographs show the As peaks (c, d and f). As contents of the Fe (hydr)oxides in the figures are provided in Table 1: (c) GS25-1, (d) GS6-4, (f) GS11-1 and (g) GS6-1.

groundwaters are seriously contaminated with As either by the reductive dissolution of Fe-(hydr)oxides or by the desorption from Fe-(hydr)oxides (Table 1). The HNO_3 extraction exhibited the As concentration range (8.8–387 mg/kg with 108 mg/kg on average; Fig. 1c) much narrower than that of the rock samples (Table 3). The highest and lowest As concentrations of the soil were much lower and higher than the respective concentrations of the rock samples, another indication that the pedogenetic process spreads the soil As contamination. The As contamination by agrochemicals such as herbicides, pesticides, additives to livestock feed, and crop desiccants [3] is unlikely in our study area because the soil samples collected from the forests (GS25 and GS11; Fig. 1c) show even higher As concentrations than other samples.

4.4. Mobilization of As by arsenopyrite oxidation (deep groundwater)

Considering that arsenopyrite is the only important As-bearing mineral in the core samples, the oxidation of arsenopyrite is the major mechanism increasing As concentrations in the deep bedrock groundwater. The pH–Eh diagram also indicates that all the groundwaters are under a condition where As(V) is stable (Fig. 7). The speciation analysis of As shows that groundwaters with low Eh levels have higher As(III) fractions (Fig. 8a). This illustrates two points

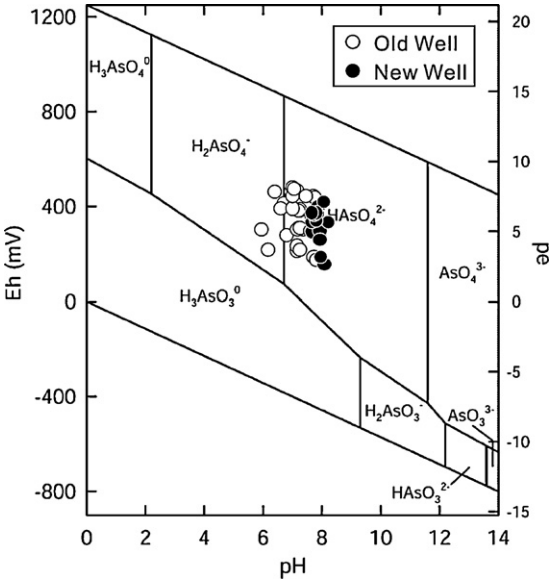

Fig. 7. The plot of groundwater samples on the pH–Eh diagram of arsenic species in the system As–O_2–H_2O at 25 °C and 1 bar total pressure [3].

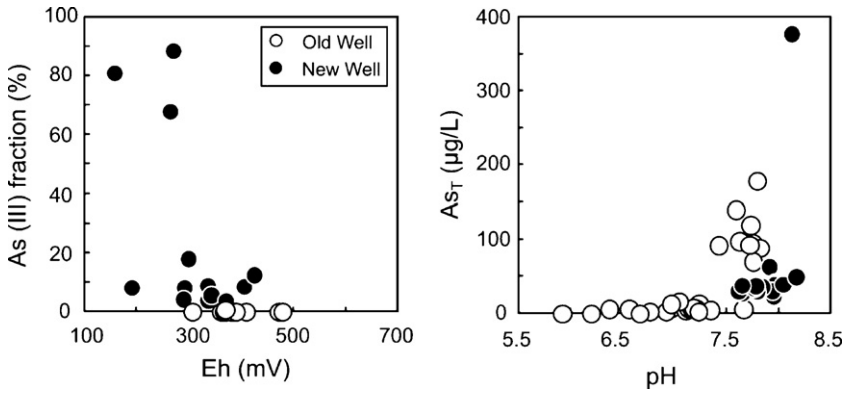

Fig. 8. Relations between As(III) fraction and Eh (a) and between As_T and pH (b).

that sulfide oxidation shifts Eh to a lower level [43] and that As is released from arsenopyrite as arsenite at the low Eh condition and transforms to arsenate as Eh increases. Under the redox condition where arsenate is stable, ferrous ions released from sulfides are also oxidized and precipitate as Fe-(hydr)oxides, the strong arsenic adsorbent [44]. Indeed, thin Fe-(hydr)oxide coatings were occasionally observed on the fracture surfaces in the core samples. The adsorption of arsenate onto the Fe-(hydr)oxides decreases as the pH increases [3,25,27], resulting in high As concentrations at high pH as Fig. 8b shows.

Considering the localized occurrence of arsenopyrite-rich veins in the roadcut, those observed from the core would also be limited to the small area around the new well. This means that the old wells may not be in direct contact with arsenopyrite-rich veins and the arsenite released from arsenopyrite has to travel some distance to reach old wells. For this case, the arsenite can be oxidized while it moves to the old wells. This, we infer, is the reason for the undetectable As(III) concentrations in the old wells (Fig. 8a; Table 2).

The high concentrations of SO_4^{2-} (10–70 mg/L) in the groundwater seem to be related to the oxidation of sulfide minerals. The oxidation of sulfides normally shifts the pH to a lower range, making the solution acidic [43]. However, the groundwater pH was generally >7 in the study area due to the dissolution of carbonate minerals in the bedrock, with several exceptions at the shallow depths (Fig. 2c). It is likely that the high pH have prevented the total removal of the As released from arsenopyrite by Fe-(hydr)oxides and played a role to some extent for the correlation between the As concentrations in the rock and in contacting groundwaters.

4.5. Mobilization of As from soils (shallow groundwater)

Because the isotope data indicate that the shallow groundwaters were recharged from the soils around the wells, they should reflect the soil composition. However, no clearly defined relationship in As distribution was observed between the soil and the shallow groundwater (Fig. 1b and c). This observation indicates that the geochemical condition is more important in mobilizing As from soils than the total As concentrations when Fe-(hydr)oxides are the main As hosts.

The high NO_3^- concentration indicates that the shallow groundwaters are not under a reducing environment that is sufficient for the reduction of Fe-(hydr)oxides. According to Kim et al. [8], nitrate strongly buffers the redox condition, and the reductive dissolution of Fe-(hydr)oxides is suppressed in the presence of nitrate. Furthermore, the shallow groundwaters showed low pH values. As a result, the shallow groundwaters are undersaturated with calcite and are high in Ca concentrations due to the greater calcite dissolution (Fig. 2). The lower pH at the shallow depth seems to be associated with fertilizers applied to the land surface [46], the oxidation of organic materials, and/or the enhanced oxidation of sulfide minerals in the soil zone, considering high NO_3^-, pCO_2, and SO_4^{2-} levels at shallow depths, respectively (Fig. 2). High sulfate concentrations in shallow groundwaters are also frequently associated with fertilizers in agricultural areas [8,45,46]. In any case, it is reasonable to infer that the low pH increased the adsorption capacity of Fe-(hydr)oxides for As, resulting in low As concentrations in the shallow groundwaters even though the soil contamination level was very serious.

In Santiago del Estero Province, Argentina, As concentrations have been reported to be 2.5–7.3 mg/kg in the aquifer materials, which are much lower than those in the soils of this study (Table 1). However, the groundwater shows As concentrations as high as 14,969 μg/L (743 μg/L on average) due to the desorption from Fe-(hydr)oxides by pH increase [25]. The pH in that area ranges from 6.4 to 9.3, and the groundwaters with As concentrations >100 μg/L show pH > 7. In our study area, the shallow groundwaters show a pH < 7 and, thus, could show low As concentrations at present.

However, the As concentration of the shallow groundwater can increase to a very high level if the pH is disturbed by land-use changes because the soil As concentrations in our study area are much higher than those observed in Argentina. For example, if the liming for mitigation of soil acidification is excessive, the pH of soil and shallow groundwater will be significantly increased [45]. Changes in cultivation would also potentially cause very high As concentrations. For example, paddy cultivation requires a waterlogged condition, which generates a strong reducing environment in the soil [47]. Fe-(hydr)oxides are dissolved under this condition and As concentration increases to a high level even though the As content of the solid phases is very low. The groundwaters in the areas, such as the Ganga–Maghna–Bramaputra Plain, the Red River Delta, the Mekong River Delta, and Inner Mongolia, where the As contents in the solid phases are much lower than those of this study, show As concentrations up to hundreds to thousands of μg/L due to the reductive dissolution of Fe-(hydr)oxides (Table 1). Therefore, keeping soils under an oxidizing, weakly acidic environment is the key in immobilizing As bound to Fe-(hydr)oxides in the soils of the study area unless active treatment is put in practice.

5. Conclusions

Very high As concentrations were observed in the bedrock and soil in the study area. The As concentrations in the bedrock are associated with arsenopyrite occurring in the veins. Due to weathering of the arsenopyrite-bearing rocks, the soils also showed very serious As contamination levels. The soils showed more dispersed As concentrations than the rock samples, indicating that pedogenetic processes have spread the As contamination. We found that the As

levels in the groundwater can be very high and that their distribution is similar to that of contacting solid phases when the oxidation of arsenopyrite occurs at high pH. Despite the high As contamination levels in the soils, the shallow groundwaters showed As concentrations generally satisfying the drinking water limit due to the adsorption onto Fe-(hydr)oxides. This was facilitated by the low pH of the shallow groundwater. However, there is a possibility that the As concentration of the shallow groundwater is increased to a very high level by the disturbances of the soil hydrogeochemical condition. Careful land planning is suggested to keep the As concentration of shallow groundwater low.

Acknowledgment

This work (#2009-0080708) was supported by Mid-career Researcher Program through the National Research Foundation grant funded by the Ministry of Education, Science and Technology.

Appendix A. Supplementary data

Supplementary data associated with this article can be found, in the online version, at doi:10.1016/j.jhazmat.2011.10.037.

References

[1] D.K. Nordstrom, Worldwide occurrences of arsenic in groundwater, Science 296 (2002) 2143–2145.
[2] D. Chakraborti, M.M. Rahman, B. Das, M. Murrill, S. Dey, S.C. Mukherjee, R.K. Dhar, B.K. Biswas, U.K. Chowdhury, S. Roy, S. Sorif, M. Selim, M. Rahman, Q. Quamruzzaman, Status of groundwater arsenic contamination in Bangladesh: a 14-year study report, Water Res. 44 (2010) 5789–5802.
[3] P.L. Smedley, D.G. Kinniburgh, A review of the source, behavior and distribution of arsenic in natural waters, Appl. Geochem. 17 (2002) 517–568.
[4] T.M. Williams, F.M. Fordyce, A. Paijitprapapon, P. Charoenchaisri, Arsenic contamination in surface drainage and groundwater in part of the South-east Asia tin belt, Nakhon si Thammarat Province Southern Thailand, Environ. Geol. 27 (1996) 16–33.
[5] D.J. Bottomley, Origins of some arseniferous groundwaters in Nova Scotia and New Brunswick, Canada, J. Hydrol. 69 (1984) 223–257.
[6] M.E. Schreiber, J.A. Simo, P.G. Freiberg, Stratigraphic and geochemical controls on naturally occurring arsenic in groundwater, eastern Wisconsin, USA, Hydrogeol. J. 8 (2000) 161–176.
[7] M.J. Kim, J. Nriagu, S. Haack, Arsenic behavior in newly drilled wells, Chemosphere 52 (2003) 623–633.
[8] K. Kim, J.T. Moon, S.H. Kim, K.S. Ko, Importance of surface geologic condition in regulating As concentration of groundwater in the alluvial plain, Chemosphere 77 (2009) 473–484.
[9] J.T. Moon, Occurrence and behaviors of arsenic in alluvial aquifer of Mankyeong River watershed, Master Thesis, Kunsan National University, Kunsan, Korea, 2009.
[10] C.F. Harvey, C.H. Swartz, A.B.M. Badruzzaman, N. Keon-Blute, W. Yu, M.A. Ali, J. Jay, R. Beckie, V. Niedan, D. Brabander, P.M. Oates, K.N. Ashfaque, S. Islam, H.F. Hemond, M.F. Ahmed, Arsenic mobility and groundwater extraction in Bangladesh, Science 298 (2002) 1602–1606.
[11] A.H.M.S. Reza, J.-S. Jean, M.-K. Lee, C.-C. Liu, J. Bundschuh, H.-J. Yang, J.-F. Lee, Y.-C. Lee, Implications of organic matter on arsenic mobilization into groundwater: evidence from northwestern (Chapai-Nawabganj), central (Manikganj) and southeastern (Chandpur) Bangladesh, Water Res. 44 (2010) 5556–5574.
[12] M.H. Bibi, F. Ahmed, H. Ishiga, Geochemical study of arsenic concentrations in groundwater of the Meghna River Delta, Bangladesh, J. Geochem. Explor. 97 (2008) 43–58.
[13] S. Kar, J.P. Maity, J.S. Jean, C.C. Liu, B. Nath, H.J. Yang, J. Bundschuh, Arsenic-enriched aquifers: occurrences and mobilization of arsenic in groundwater of Ganges Delta Plain, Barasat, West Bengal, India, Appl. Geochem. 25 (2010) 1805–1814.
[14] P. Bhattacharyya, S. Tripathy, K. Kim, S.H. Kim, Arsenic fractions and enzyme activities in arsenic-contaminated soils by groundwater irrigation in West Bengal, Ecotoxicol. Environ. Saf. 71 (2008) 149–156.
[15] A. Mukherjee-Goswami, B. Nath, J. Jana, S.J. Sahu, M.J. Sarkar, G. Jacks, P. Bhattacharya, A. Mukherjee, D.A. Polya, J.S. Jean, D. Chatterjee, Hydrogeochemical behavior of arsenic-enriched groundwater in the deltaic environment: comparison between two study sites in West Bengal, India, J. Contam. Hydrol. 99 (2008) 22–30.
[16] J.K. Gurung, H. Ishiga, M.S. Khadka, Geological and geochemical examination of arsenic contamination in groundwater in the Holocene Terai Basin, Nepal, Environ. Geol. 49 (2005) 98–113.
[17] M. Berg, P.T.K. Trang, C. Stengel, J. Buschmann, P.H. Viet, N.V. Dan, W. Giger, D. Stüben, Hydrological and sedimentary controls leading to arsenic contamination of groundwater in the Hanoi area, Vietnam: the impact of iron-arsenic ratios, peat, river bank deposits, and excessive groundwater abstraction, Chem. Geol. 249 (2008) 91–112.
[18] P.L. Smedley, M. Zhang, G. Zhang, Z. Luo, Mobilisation of arsenic and other trace elements in fluviolacustrine aquifers of the Huhhot Basin, Inner Mongolia, Appl. Geochem. 18 (2003) 1453–1477.
[19] H. Guo, S. Yang, X. Tang, Y. Li, Z. Shen, Groundwater geochemistry and its implications for arsenic mobilization in shallow aquifers of the Hetao Basin, Inner Mongolia, Sci. Total Environ. 393 (2008) 131–144.
[20] K.Y. Chen, T.K. Liu, Major factors controlling arsenic occurrence in the groundwater and sediments of the Chianan coastal plain, SW Taiwan, Terr. Atmos. Ocean. Sci. 18 (2007) 975–994.
[21] B. Nath, J.S. Jean, M.K. Lee, H.J. Yang, C.C. Liu, Geochemistry of high arsenci groundwater in Chia-Nan plain Southwestern Taiwan: possible sources and reactive transport of arsenic, J. Contam. Hydrol. 99 (2008) 85–96.
[22] A.H.M. Selim Reza, J.S. Jean, H.J. Yang, M.K. Lee, B. Woodall, C.C. Liu, J.F. Lee, S.D. Luo, Occurrence of arsenic in core sediments and groundwater in the Chapai-Nawabganj District, northwestern Bangladesh, Water Res. 44 (2010) 2021–2037.
[23] K.P Naguyen, R. Itoi, Source and release mechanism of arsenic in aquifers of the Mekong Delta, Vietnam, J. Contam. Hydrol. 103 (2009) 58–69.
[24] A.H. Welch, M.S. Lico, Factors controlling As and U in shallow ground water, southern Carson Desert, Nevada, Appl. Geochem. 13 (1998) 521–539.
[25] P. Bhattacharya, M. Claesson, J. Bundschuh, O. Sracek, J. Fagerberg, G. Jacks, R.A. Martin, A.R. Storniolo, J.M. Thir, Distribution and mobility of arsenic in the Río Dulce alluvial aquifers in Santiago del Estero Province, Argentina, Sci. Total Environ. 358 (2006) 97–120.
[26] R.T. Nickson, J.M. McArthur, P. Ravenscroft, W.G. Burgess, K.M. Ahmed, Mechanism of arsenic release to groundwater, Bangladesh and West Bengal, Appl. Geochem. 15 (2000) 403–413.
[27] S. Dixit, J.G. Hering, Comparison of arsenic (V) and arsenic (III) sorption onto iron oxide minerals: implications for arsenic mobility, Environ. Sci. Technol. 37 (2003) 4182–4189.
[28] S.H. Hong, W.C. Choi, The Geological Map of Geumsan Sheet (Scale 1:50 000) with Explanatory Text, Korea Research Institute of Geoscience and Mineral Resources, 1978 (in Korean).
[29] C.W. Fetter, Applied Hydrogeology, 3rd ed., Prentice Hall, Englewood Cliffs, New Jersey, 1994.
[30] Rural Development Administration of Korea. Soil Environment Information System. http://www.rda.go.kr/.
[31] Korea Meteorological Administration, Databases for the Annual Climatological Reports. http://www.kma.go.kr/weather/observation/data_monthly.jsp.
[32] X. Meng, W. Wang, Speciation of arsenic by disposable cartridges, in: Proceedings of the Third International Conference on Arsenic Exposure and Health Effects, July 12–15, San Diego, CA, 1998.
[33] I.D. Clark, P. Fritz, Environmental Isotopes in Hydrogeology, Lewis Publishers, New York, 1997, 328 pp.
[34] J.I. Drever, Geochemistry of Natural Waters: The Surface and Groundwater Environments, 3rd ed., Prentice-Hall Inc., Englewood Cliffs, NJ, 1997.
[35] D.L. Parkhurst, C.A.J. Appelo, User's guide to PHREEQC (version 2)—A Computer Program for Speciation, Batch-Reaction, One-Dimesnional Transport, and Inverse Geochemical Calculations, USGS Water-resources Investigations Report 99-4259, 1999.
[36] K. Kim, M.H. Koo, S.H. Moon, B.W. Yum, K.S. Lee, Hydrochemistry of groundwaters in a spa area of Korea: an implication for water quality degradation by intensive pumping, Hydrol. Process. 19 (2005) 493–505.
[37] K. Kim, G.Y. Jeong, Factors influencing the occurrence of fluoride-rich groundwaters: a case study in the southeastern part of the Korean Peninsula, Chemosphere 58 (2005) 1399–1408.
[38] J.M. Bigham, D.K. Nordstrom, Iron and aluminum hydroxysulfates from acid sulfate waters, Rev. Mineral. Geochem. 40 (2000) 351–403.
[39] U. Schwertmann, L. Carlson, The pH-dependent transformation of schwertmannite to goethite at 25 °C, Clays Clay Miner. 40 (2005) 63–66.
[40] L. Carlson, J.M. Bigham, U. Schwertmann, A. Kyek, F. Wagner, Scavenging of As from acid mine drainage by schwertmannite and ferrihydrite: a comparison with synthetic analogues, Environ. Sci. Technol. 36 (2002) 1712–1719.
[41] K. Fukushi, T. Sato, N. Yanase, J. Minato, H. Yamada, Arsenate sorption on schwertmannite, Am. Mineral. 89 (2004) 1728–1734.
[42] S. Regenspurg, S. Peiffer, Arsenate and chromate incorporation in schwertmannite, Appl. Geochem. 20 (2005) 1226–1239.
[43] C.A.J. Appelo, D. Postma, Geochemistry Groundwater and Pollution, 2nd ed., CRC Press, Boca Raton, FL, 2005.
[44] M.C. Campbell, D. Malasarn, C.W. Saltikov, D.K. Newman, J.G. Hering, Simultaneous microbial reduction of iron(III) and arsenic(V) in suspensions of hydrous ferric oxide, Environ. Sci. Technol. 40 (2006) 5950–5955.
[45] G.T. Chae, K. Kim, S.T. Yun, K.H. Kim, S.O. Kim, B.Y. Choi, H.S. Kim, C.W. Rhee, Hydrogeochemistry of alluvial groundwaters in an agricultural area: an implication for groundwater contamination susceptibility, Chemosphere 55 (2004) 369–378.
[46] K. Kim, H.J. Kim, B.Y. Choi, S.H. Kim, K.H. Park, E. Park, D.C. Koh, S.T. Yun, Fe and Mn levels regulated by agricultural activities in alluvial groundwaters underneath a flooded paddy field, Appl. Geochem. 23 (2008) 44–57.
[47] Y. Takahashi, R. Minamikawa, K.H. Hattori, K. Kurishima, N. Kihou, K. Yuita, Arsenic behavior in paddy fields during the cycle of flooded and non-flooded periods, Environ. Sci. Technol. 38 (2004) 1038–1044.